UNIVERSITY of York

This is a repository copy of *Analysis and Compensation of Sampling Errors in TPFS IPMSM Drives With Single Current Sensor*.

White Rose Research Online URL for this paper:
https://eprints.whiterose.ac.uk/162733/

Version: Accepted Version

Article:
lu, jiadong, Hu, Yihua and Liu, Jinglin (2019) Analysis and Compensation of Sampling Errors in TPFS IPMSM Drives With Single Current Sensor. IEEE Transactions on Industrial Electronics. pp. 3852-3855. ISSN 0278-0046

https://doi.org/10.1109/TIE.2018.2838114

Reuse
Items deposited in White Rose Research Online are protected by copyright, with all rights reserved unless indicated otherwise. They may be downloaded and/or printed for private study, or other acts as permitted by national copyright laws. The publisher or other rights holders may allow further reproduction and re-use of the full text version. This is indicated by the licence information on the White Rose Research Online record for the item.

Takedown
If you consider content in White Rose Research Online to be in breach of UK law, please notify us by emailing eprints@whiterose.ac.uk including the URL of the record and the reason for the withdrawal request.

White Rose university consortium
Universities of Leeds, Sheffield & York

eprints@whiterose.ac.uk
https://eprints.whiterose.ac.uk/

Analysis and Compensation of Sampling Errors in TPFS IPMSM Drives with Single Current Sensor

Jiadong Lu, Yihua Hu, *Senior Member, IEEE,* Jinglin Liu, *Member, IEEE*

***Abstract*—The current reconstruction strategies using single current sensor in the motor drives are widely researched. However, the sampled currents do not represent the average values within the modulation period, especially for the asymmetric modulation or asymmetric sampling solutions. This is due to the following two reasons: 1) the detected current values obtained at different sampling points are utilized to calculate the three-phase currents; 2) the detected instantaneous currents are applied to estimate the average current values. In this paper, the current change rates under different action vectors are estimated to compensate these errors in a three-phase four-switch (TPFS) interior permanent magnet synchronous motor (IPMSM) drive with single current sensor. The effectiveness of the proposed strategy is verified by experimental results on a 5kW IPMSM motor prototype, which shows that the current reconstruction errors are reduced after compensation.**

***Index Terms*—Current sampling error, interior permanent magnet synchronous motor (IPMSM), phase current reconstruction, pulse width modulation**

I. Introduction

THE accuracy of three-phase currents is a matter of significance for an interior permanent magnet synchronous motor (IPMSM) speed control system. The three-phase currents are usually measured by the three-phase current sensors. Take reliability and cost efficiency into consideration, the three-phase four-switch (TPFS) inverter topology [1] (as illustrated in Fig.1) and phase current reconstruction strategies [2], [3] are proposed. Because the average phase currents are commonly utilized in the control system, the current oversampling technology is applied [4]. However, the phase current reconstruction strategies utilize only one current sensor and are combined with PWM signals, which makes it difficult to obtain the average three-phase current values using oversampling methods.

Manuscript received October 24, 2017; revised January 26, 2018 and April 10, 2018; accepted May 5, 2018. This work was supported by Shaanxi Science Technology Co-ordination and Innovation Project, China (2013KTCQ01-20, 2016KTCQ01-49). *(Corresponding author: Jinglin Liu).*

J. Lu and J. Liu are with the School of Automation, Northwestern Polytechnical University, and Shaanxi Key Laboratory of Small & Special Electrical Machine and Drive Technology, Xi'an 710129, China. (E-mail: noodle@mail.nwpu.edu.cn, jinglinl@nwpu.edu.cn).

Y. Hu is with the Department of Electrical Engineering and Electronics, University of Liverpool, Liverpool L69 3GJ, U.K. (E-mail: y.hu35@liverpool.ac.uk).

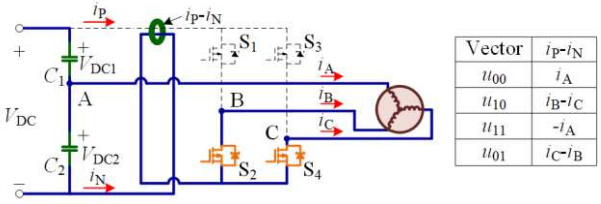

Vector	i_P-i_N
u_{00}	i_A
u_{10}	i_B-i_C
u_{11}	-i_A
u_{01}	i_C-i_B

Fig. 1. Topology of the IPMSM drive fed by TPFS inverter with current reconstruction strategy (action vector: u_{00}).

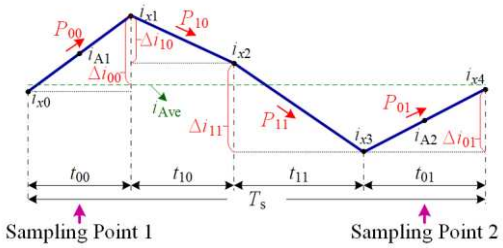

Fig. 2. Current of phase-A within one PWM cycle.

The current sampling errors in the motor drives have been studied over the years [4] - [6]. In [4], the errors of linear current approximation in high-speed operations are analyzed, even when the midpoint sampling method of the symmetric pulse width modulation (PWM) is applied. This kind of error is usually called the PWM-induced ripple [5]. The impact of current sensor errors on system performance are analyzed in [6], which mainly considered the DC-offset and scaling errors.

For the single current sensor based drives, different current sampling errors can be caused according to the types of PWM and sampling methods. In the case of asymmetrical PWM generation or asymmetrical sampling, there are two kinds of sampling errors: (1) Calculation of the three-phase currents with sampled values from different sampling points (defined as "Error 1"); (2) Estimation of the average current values with the detected instantaneous ones (defined as "Error 2"). The current sampling errors would lead to speed fluctuation and torque ripple, which should be carefully studied [6]. In the case of symmetric PWM with midpoint sampling method for current reconstruction strategies using single current sensor, the aforementioned errors are not presented. However, the circuit

topology needs to be changed [3]. In this paper, the sampling errors of a TPFS inverter fed IPMSM drive with one current sensor is studied (as displayed in Fig.1). The three-phase current values are obtained according to the sampled currents derived by applying two adjacent vectors. In the figure, there are four switching states, and the detected current i_P-i_N has the same value with those of i_A, i_B-i_C, -i_A, and i_C-i_B when applying the action vectors u_{00}, u_{10}, u_{11}, and u_{01} respectively. The PWM type and sampling method are all asymmetrical ones, as illustrated in Fig.2.

II. Sampling Errors of Current Reconstruction Strategy in TPFS Inverter Fed IPMSM Drives

In Fig.2, the reconstructed phase-A current i_A' is obtained at sampling point 1 (i_1), which is also utilized to calculate the reconstructed phase-B and -C currents i_B' and i_C' at sampling point 2. However, the value of i_A' keeps changing within the whole PWM cycle [5], and this would bring "Error 1" to the current reconstruction processes of i_B' and i_C'. "Error 1" can be eliminated by using the independent current reconstruction strategy [2], but a special type of PWM is required, and "Error 2" still exists, which is caused by applying the detected instantaneous current values to estimate the average ones. In Fig.2, P_{00}, P_{10}, P_{11} and P_{01} represent the current change rates when applying the vectors u_{00}, u_{10}, u_{11} and u_{01}, respectively. i_{Ave} denotes the average current value within the whole PWM cycle. i_{A1}, i_{B1}, and i_{C1} are the actual three-phase currents at sampling point 1, whereas i_{A2}, i_{B2}, and i_{C2} are the actual values at sampling point 2.

In Fig.2, i_{A1} and i_{A2} are not equal, and the difference Δi_{A12} and "Error 1" can be described as

$$\begin{cases} \Delta i_{A12}=i_{A2}-i_{A1}=\Delta i_{00}/2+\Delta i_{10}+\Delta i_{11}+\Delta i_{01}/2 \\ i_A'=i_{A1}=i_{A2}-\Delta i_{A12} \\ i_B'=i_{B2}+\Delta i_{A12}/2 \\ i_C'=i_{C2}+\Delta i_{A12}/2 \end{cases} \tag{1}$$

where i_A', i_B', and i_C' are the reconstructed three-phase currents.

From (1), it can be concluded that i_A' is the same with the actual phase-A current at sampling point 1. i_B' and i_C' are equal to the actual phase-B, -C currents at sampling point 2 with the same additional component $\Delta i_{A12}/2$. Because the four current increments Δi_{00}, Δi_{10}, Δi_{11}, and Δi_{01} in Fig.2 are not constant values, the values of "Error 1" are not constant as well.

In Fig.2, the average value i_{Ave} is not equal to i_A', which can be referred as "Error 2". The same error also exists in phase-B and -C currents

$$\begin{cases} i_A'=i_{A1}=i_{x0}+P_{00}\cdot t_{00}/2 \\ i_{Ave}=t_{00}/T_s\cdot(i_{x0}+i_{x1})/2+t_{10}/T_s\cdot(i_{x1}+i_{x2})/2 \\ \quad +t_{11}/T_s\cdot(i_{x2}+i_{x3})/2+t_{01}/T_s\cdot(i_{x3}+i_{x4})/2 \end{cases}. \tag{2}$$

III. Proposed Compensation Scheme

The mathematical model of IPMSM is given by [2]

$$\begin{bmatrix} u_\alpha \\ u_\beta \end{bmatrix}=R\cdot\begin{bmatrix} i_\alpha \\ i_\beta \end{bmatrix}+\boldsymbol{L}\cdot\frac{\mathrm{d}}{\mathrm{d}t}\begin{bmatrix} i_\alpha \\ i_\beta \end{bmatrix}+\omega\cdot\begin{bmatrix} -\psi_\beta \\ \psi_\alpha \end{bmatrix} \tag{3}$$

$$\begin{bmatrix} \psi_\alpha \\ \psi_\beta \end{bmatrix}=2L_2\cdot\begin{bmatrix} \cos 2\theta & \sin 2\theta \\ \sin 2\theta & -\cos 2\theta \end{bmatrix}\cdot\begin{bmatrix} i_\alpha \\ i_\beta \end{bmatrix}+\psi_f\cdot\begin{bmatrix} \cos\theta \\ \sin\theta \end{bmatrix} \tag{4}$$

$$\boldsymbol{L}=\begin{bmatrix} L_0+L_2\cos(2\theta) & L_2\sin(2\theta) \\ L_2\sin(2\theta) & L_0-L_2\cos(2\theta) \end{bmatrix} \tag{5}$$

$$\begin{cases} L_0=(L_d+L_q)/2>0 \\ L_2=(L_d-L_q)/2<0 \end{cases} \tag{6}$$

where u_α, u_β and i_α, i_β are the motor voltages and currents in the Clark reference frame, respectively; R is the motor resistance; L_d and L_q are the d- and q-axis stator inductances; θ is the rotor position; ω is the motor speed; ψ_f is the flux linkage of the permanent magnet.

The current change rates can be obtained

$$\begin{bmatrix} di_\alpha/dt \\ di_\beta/dt \end{bmatrix}=\boldsymbol{L}^{-1}\cdot\begin{bmatrix} u_\alpha-Ri_\alpha+\omega\psi_\beta \\ u_\beta-Ri_\beta-\omega\psi_\alpha \end{bmatrix}. \tag{7}$$

Usually u_α and u_β are much bigger than $Ri_{\alpha/\beta}$ and $\omega\psi_{\alpha/\beta}$ in low speed conditions, and the current change rates can be simplified as (8). It is worth noting that the current change rates in (8) achieve higher accuracy in the low-speed mode. For high speed conditions, the current change rates can be estimated by using (7).

$$\begin{bmatrix} di_\alpha/dt \\ di_\beta/dt \end{bmatrix}=\boldsymbol{L}^{-1}\cdot\begin{bmatrix} u_\alpha \\ u_\beta \end{bmatrix}. \tag{8}$$

In (7) and (8) u_α and u_β are related to the switching states and can be calculated with 3/2 transform from equation (1) in [1]

$$\begin{bmatrix} u_\alpha \\ u_\beta \end{bmatrix}=\begin{bmatrix} -1/\sqrt{6} & -1/\sqrt{6} \\ 1/\sqrt{2} & -1/\sqrt{2} \end{bmatrix}\begin{bmatrix} S_bV_{DC1}-(1-S_b)V_{DC2} \\ S_cV_{DC1}-(1-S_c)V_{DC2} \end{bmatrix} \tag{9}$$

S_b and S_c denote the switching states in Fig.1, where "1" represents the closing state of the upper switch in the corresponding bridge arm, whereas "0" represents closing state of the lower switch in the corresponding bridge arm.

In (8), by applying 2/3 transformation, the three-phase current change rates by applying different vectors can be deduced, e.g., P_{00}, P_{10}, P_{11} and P_{01} for i_A in Fig.2. Therefore the current change rate of i_A together with i_A' can be utilized to calculate the five values in Fig.2, i.e., i_{x0}, ..., i_{x4}. Because the action time of the four vectors is pre-set, the average current value i_{A_Ave} can be finally obtained by using (2). For phase-B and -C, the calculation methods are similar. It is worth noting that (2) varies with the distribution of two sampling points according to the output voltage vector.

IV. Verification

In order to verify the existence of the errors in current reconstruction strategies and the effectiveness of the proposed compensation scheme, the experiment is carried out on a 5 kW IPMSM prototype. The main parameters of the IPMSM are displayed in Table I. The PWM synthesis strategy is set independently from the vector sectors, i.e., $u_{00}\rightarrow u_{10}\rightarrow u_{11}\rightarrow u_{01}$.

TABLE I
MAIN PARAMETERS OF IPMSM FOR EXPERIMENT.

Parameter	Value	Parameter	Value
Rated power	5 kW	Pole pairs	3
Rated voltage	380 V	d-axis Inductance	4.2 mH
Rated current	8.5 A	q-axis Inductance	10.1 mH
Rated torque	15 N·m	Phase resistance	0.18 Ω
Switching frequency	8 kHz	Maximum speed	3000 r/min
Dead time	4 μs	DC-link voltage	540 V

TABLE II
CURRENT CHANGE RATES AND ACTION TIME OF FOUR VECTORS IN FIG.3.

Variable	Phase-A	Phase-B	Phase-C
P_{00}	22237 A/s	-2987 A/s	-19251 A/s
P_{10}	19330 A/s	49824 A/s	-66153 A/s
P_{11}	-21749 A/s	2921 A/s	18828 A/s
P_{01}	-15841 A/s	-49889 A/s	65731 A/s
t_{00}	26.18 us	t_{10}	31.47 us
t_{11}	36.91 us	t_{01}	30.44 us

The voltage sectors are the same as those defined in [1].

Fig.3 shows the detected and actual three-phase currents (here, θ=66°). The two sampled currents are respectively $i_1=i_{B1}$-i_{C1}=4.14 A and i_2=-i_{A2}=5.00 A (the distribution of the two sampling points varies with vector sectors). Therefore, the reconstructed three-phase currents can be calculated as i_A'=-i_2=-5.00 A, $i_B'=(i_1+i_2)/2$=4.57 A and $i_C'=(-i_1+i_2)/2$=0.43 A. The average three-phase currents are measured as i_{A_Ave}=-5.20 A, i_{B_Ave}=4.61 A and i_{C_Ave}=0.59 A. It can be seen that the errors of the reconstructed three-phase currents are 0.20 A, -0.04 A, -0.16 A, respectively.

In order to compensate the errors, the current change rates for the three-phase currents calculated by using (8) and (9) with 2/3 transformation are displayed in Table II. The action time of the four basic vectors is also shown in Table II. With all the data in Table II, all the five values in Fig.2, i.e., i_{x0}, ..., i_{x4} for the three-phase currents can be obtained. Finally, the values of three-phase currents after compensation can be calculated, where i_{A_Com}'=-5.24 A, i_{B_Com}'=4.65 A, i_{C_Com}'=0.61 A. The errors are respectively -0.04 A, 0.04 A, 0.02 A, which are significantly reduced.

In Fig.4, the average and reconstructed three-phase currents before and after compensation in the steady state are illustrated. In the figure, i_A, i_B, i_C and i_{A_Ave}, i_{B_Ave}, i_{C_Ave} are the actual and average three-phase currents, respectively; i_A', i_B', i_C' and i_{A_Com}', i_{B_Com}', i_{C_Com}' are the reconstructed three-phase currents before and after compensation of both "Error 1" and "Error 2", respectively. The total harmonic distribution (THD) value of the average current is 1.36%, and the value of the reconstructed current before compensation is 6.49%, and it becomes 2.49% after compensation. The error of the reconstructed phase currents before compensation is about ±0.35 A (5.8%), whereas it is ±0.09 A (1.5%) after compensation.

Fig.5 shows the average and reconstructed three-phase currents before and after compensation in the dynamic process. It can be seen that the errors are reduced after compensation even in the fast dynamic process.

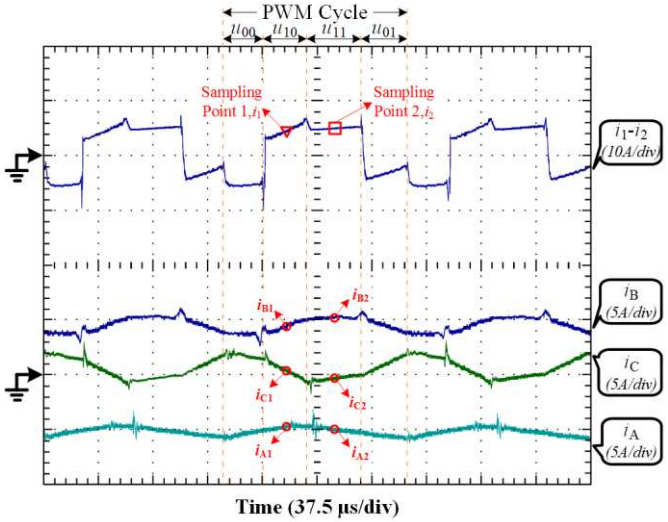

Fig. 3. Detected currents and three-phase currents.

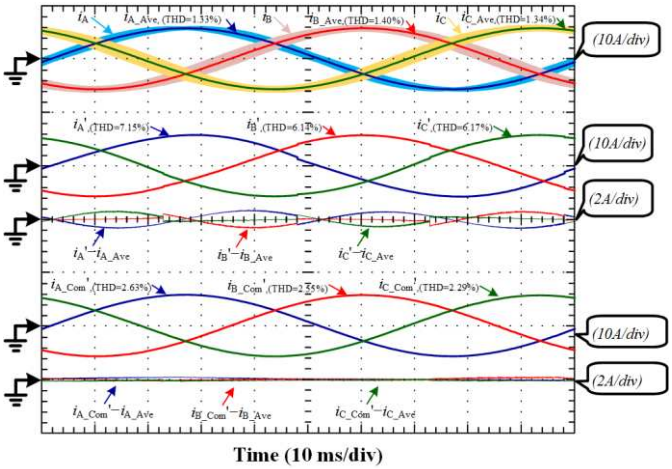

Fig. 4. Average and reconstructed three-phase currents before and after compensation (200 rpm).

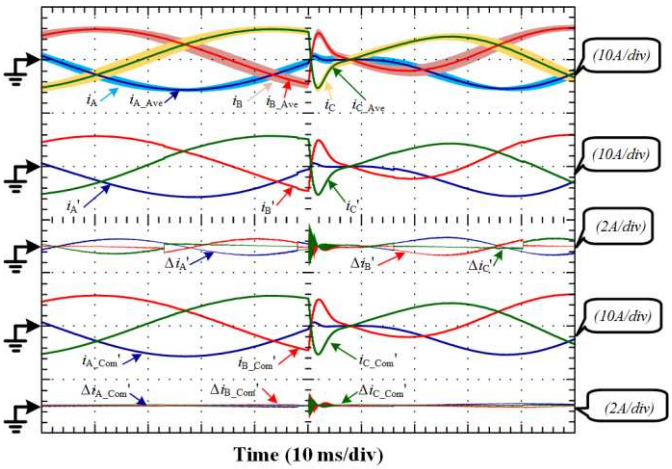

Fig. 5. Experimental results of three-phase currents in dynamic states.

V. CONCLUSION

In this paper, the sampling errors of current reconstruction strategies in IPMSM drives are studied. It is found that the

reconstructed three-phase current values have two kinds of errors, which are compensated by using the estimated current change rates in this paper. The existence of the errors and the effectiveness of the proposed compensation scheme are verified by the experiment on a 5 kW IPMSM prototype. It is worth noting that the analysis and compensation strategy introduced in this paper are also widely applicable in a three-phase six-switch (TPSS) inverter if an asymmetrical PWM strategy or asymmetrical sampling method is utilized. The compensation strategy of phase current reconstruction sampling errors achieves high accuracy under low-speed and light-load conditions. This is because in (8) the resistance voltage drop and the term related to motor speed in (7) are ignored for simplification. When working under high-speed or heavy-load conditions, the accuracy lightly decreases. However, if higher estimation accuracy of the current change rate is needed, (7) should be utilized. However, the algorithm complexity and computational burden are increased.

REFERENCES

[1] Z. Y. Zeng, W. Y. Zheng, and R. X. Zhao, “Performance analysis of the zero-voltage vector distribution in three-phase four-switch converter using a space vector approach,” *IEEE Trans. Power Electron.*, vol. 32, no. 1, pp. 260-273, Jan., 2017.

[2] J. D. Lu, X. K. Zhang, Y. H. Hu, J. L. Liu, C. Gan, and Z. Wang, "Independent phase current reconstruction strategy for IPMSM sensorless control without using null switching states," *IEEE Trans. Ind. Electron.,* vol. 65, no. 6, pp. 4492-4502, June 2018.

[3] Y. X. Xu, H. Yan, J. B. Zou, B. C. Wang, and Y. H. Li, "Zero voltage vector sampling method for PMSM three-phase current reconstruction using single current sensor," *IEEE Trans. Power Electron.,* vol. 32, no. 5, pp. 3797-3807, May, 2017.

[4] L. Jarzebowicz, “Errors of a linear current approximation in high-speed PMSM drives,” *IEEE Trans. Power Electron.*, vol. 32, no. 11, pp. 8254-8257, Nov., 2017.

[5] C. M. Wolf, M. W. Degner, and F. Briz, "Analysis of current sampling errors in PWM VSI drives," *IEEE Trans. Ind. Appl.,* vol. 51, no. 2, pp. 1551-1560, Mar./Apr., 2015.

[6] F. R. Salmasi, “A self-healing induction motor drive with model free sensor tampering and sensor fault detection, isolation, and compensation,” *IEEE Trans. Ind. Electron.*, vol. 64, no. 8, pp. 6105-6115, Aug., 2017.